Neurobiology of Disease

Mutational Analysis Establishes a Critical Role for the N Terminus of Fragile X Mental Retardation Protein FMRP

Simon P. Reeve,[1,2]* Xinda Lin,[3]* Bahar H. Sahin,[4] Fangfang Jiang,[3] Aiyu Yao,[3] Zhihua Liu,[3] Hui Zhi,[3] Kendal Broadie,[5] Wei Li,[3] Angela Giangrande,[4] Bassem A. Hassan,[1,2,6] and Yong Q. Zhang[3]

[1]Laboratory of Neurogenetics, Department of Molecular and Developmental Genetics, Flanders Institute for Biotechnology and [2]Department of Human Genetics, KU Leuven School of Medicine, 3000 Leuven, Belgium, [3]Key Laboratory of Molecular and Developmental Biology, Institute of Genetics and Developmental Biology, Chinese Academy of Sciences, Beijing 100101, China, [4]Institut de Génétique et de Biologie Moléculaire et Cellulaire, Centre National de la Recherche Scientifique/Inserm/Université Louis Pasteur, 67404 Illkirch, Strasbourg, France, [5]Department of Biological Sciences, Kennedy Center for Research on Human Development, Vanderbilt University, Nashville, Tennessee 37232, and [6]Doctoral Programs in Molecular and Developmental Genetics and Neuroscience, Katholieke Universiteit Leuven Group Biomedicine, 3000 Leuven, Belgium

Fragile X syndrome is the most common form of heritable mental retardation caused by the loss of function of the fragile X mental retardation protein FMRP. FMRP is a multidomain, RNA-binding protein involved in RNA transport and/or translational regulation. However, the binding specificity between FMRP and its various partners including interacting proteins and mRNA targets is essentially unknown. Previous work demonstrated that dFMRP, the *Drosophila* homolog of human FMRP, is structurally and functionally conserved with its mammalian counterparts. Here, we perform a forward genetic screen and isolate 26 missense mutations at 13 amino acid residues in the dFMRP coding *dfmr1*. Interestingly, all missense mutations identified affect highly conserved residues in the N terminal of dFMRP. Loss- and gain-of-function analyses reveal altered axonal and synaptic elaborations in mutants. Yeast two-hybrid assays and *in vivo* analyses of interaction with CYFIP (cytoplasmic FMR1 interacting protein) in the nervous system demonstrate that some of the mutations disrupt specific protein–protein interactions. Thus, our mutational analyses establish that the N terminus of FMRP is critical for its neuronal function.

Key words: **fragile X syndrome; mental retardation; FMRP; yeast two-hybrid; *Drosophila*; *dfmr1***

Introduction

The absence of the fragile X mental retardation protein FMRP leads to fragile X syndrome (FraX). Although most FraX cases result from dynamic expansions of CGG repeats in the 5′ regulatory of *FMR1*, thus silencing its transcription and producing no protein product (O'Donnell and Warren, 2002), genomic deletions or point mutations in *FMR1* also cause rare cases of FraX (De Boulle et al., 1993; Hammond et al., 1997), emphasizing that understanding the basic molecular and cellular functions of FMRP is a prerequisite to elucidating the pathogenesis of FraX.

FMRP is a multidomain, RNA-binding protein involved in the regulation of RNA transport/translation and predicted to bind 2–4% of the mouse transcriptome (Brown et al., 2001). In addition to RNA binding capability, FMRP binds directly to a large group of proteins, including its two paralogs fragile X-related proteins 1 and 2 (FXR1 and FXR2) (Zhang et al., 1995; Siomi et al., 1996). Other interactors include NUFIP (nuclear fragile X mental retardation protein interacting protein) (Bardoni et al., 1999), 82-FIP (82 kDa FMRP interacting protein) (Bardoni et al., 2003), CYFIP1 (cytoplasmic FMR1 interacting protein 1) and CYFIP2 (Schenck et al., 2001, 2003), and MSP58 (microspherule protein 58 kDa) (Davidovic et al., 2006). However, what mediates the binding specificity between FMRP and each of these partners is essentially unknown. Although the significance of these interactions in the pathogenesis of FraX remains to be demonstrated, at least one partner CYFIP appears to contribute to the mutant phenotypes (Schenck et al., 2003).

Mouse models of FraX have contributed substantially to our current understanding of the disease (Koekkoek et al., 2005). However, the mouse model has the limitation of being inefficient for genetic screens. To apply simpler genetic approaches, we and others developed a *Drosophila* model of the disease (Zhang et al., 2001; Dockendorff et al., 2002; Morales et al., 2002; Michel et al.,

Received July 23, 2007; revised Jan. 17, 2008; accepted Feb. 3, 2008.

X.L. is supported by a postdoctoral fellowship from the Fragile X Research Foundation. This work is supported by Flanders Interuniversity Institute for Biotechnology (VIB) and a Johnson and Johnson's Corporate Office of Science and Technology/VIB proof-of-concept fund (S.P.R., B.A.H.), a Fragile X Research Foundation Grant (A.G.), and an Inserm fellowship (B.H.S.). Work in the laboratory of A.G. is supported by Centre National de la Recherche Scientifique, Inserm, and the Hôpital Universitaire de Strasbourg. This work was also supported by National Science Foundation of China (NSFC) Grant 30525007 and Chinese Academy of Sciences (CAS) Grant KSCX1-YW-R-59 (W.L.), and NSFC Grants 30430250 and 30525015, Ministry of Science and Technology of China Grants 2006AA02Z166 and 2007CB947200, and CAS Grant KSCX1-YW-R-69 (Y.Q.Z.). We are grateful to Bloomington Stock Center (Bloomington, IN) for fly stocks, Developmental Studies Hybridoma Bank (University of Iowa, Iowa City, IA) for antibodies, and C. Li and L. Zhao for assistance in sequencing the mutants. We thank our colleagues Drs. Z. Wang and X. Huang for critical reading of this manuscript and H. Siomi for cDNA clone of human *FXR1*.

*S.P.R. and X.L. contributed equally to this work.

Correspondence should be addressed to Dr. Yong Q. Zhang, Institute of Genetics and Developmental Biology, Chinese Academy of Science, Datun Road, Chaoyang District, Beijing 100101, China. E-mail: yqzhang@genetics.ac.cn.

DOI:10.1523/JNEUROSCI.5528-07.2008

 0270-6474/08/283221-06$15.00/0

2004; Pan et al., 2004). The fly *FMR1* homolog *dfmr1* shows high sequence conservation with its mammalian counterparts, and the neuronal phenotypes in the mutant flies are similar but more pronounced than those of human patients and knock-out mice (Zhang and Broadie, 2005; Leyssen and Hassan, 2007). To further dissect the structure/function relationship of FMRP, we took advantage of the power of *Drosophila* genetics and performed a large-scale mutagenesis screen for mutations in *dfmr1*. From a simple F1 screen based on the rescue of overexpression-induced lethality, we isolated 101 individual viable suppressor lines, of which 57 lines have 58 mutations in *dfmr1* (one has a double hit). Interestingly, all point mutations identified affect highly conserved residues in the N terminal of dFMRP. Yeast two-hybrid (Y2H) assays and *in vivo* analyses of interaction with CYFIP in the nervous system demonstrate that the FMRP N terminus and the specific protein–protein interactions it mediates are critical for its neuronal functions.

Materials and Methods

Drosophila *husbandry and stocks.* All *Drosophila* stocks were raised at 25°C on standard cornmeal agar media. Ubiuitously expressed *Tub–Gal4* was from Bloomington Stock Center (Bloomington, IN). Pigment dispersing factor (*Pdf*)–*Gal4* was from P. Taghert (Washington University School of Medicine, St. Louis, MO). Recombinant tool stock *Tub–Gal4, dfmr1*^{50M}*/TM6C* was constructed using conventional genetic techniques. *dfmr1*^{3}, *dfmr1*^{113}, *dfmr1*^{50M}, *EP3517*, *UAS–dfmr1*, and *UAS–CYFIP* were described previously (Zhang et al., 2001; Dockendorff et al., 2002; Morales et al., 2002; Schenck et al., 2003).

Chemical mutagenesis. Chemical mutagenesis was performed essentially as described by Grigliatti (1998). Isogenized male flies carrying *EP3517* were mutagenized with 25 mM ethyl methanesulfonate in 1% sugar. After recovery on fresh food, the mutagenized flies were mated to virgins of *Tub–Gal4/TM6C* (supplemental Fig. 1, available at www.jneurosci.org as supplemental material).

DNA sequencing. Genomic DNA of each mutant of *EP3517*/dfmr1*^{3} [* indicates a putative mutation in the endogenous *dfmr1*; *dfmr1*^{3} is a null allele of *dfmr1* with the coding region completely deleted (revised information from Dockendorff et al., 2002)] was prepared from single adult fly. PCR was then performed on the prepared DNA using five sets of primers designed to cover the genomic region encoding the full-length *dfmr1* cDNA. Sequencing results were compared with the deposited *dfmr1* sequence (GenBank accession number 205597).

Immunohistochemical analyses and Western blot analyses. Dissection and antibody staining of third-instar larvae were described previously (Zhang et al., 2001). Monoclonal anti-dFMRP 6A15 was from Sigma (St. Louis, MO) (Wan et al., 2000) and used at 1:2000; an alternative anti-dFMRP 5A11 (1:1000) was from the Developmental Studies Hybridoma Bank (University of Iowa, Iowa City, IA). For Western blot analyses, whole fly heads were homogenized in standard loading buffer and subjected to SDS-PAGE. Equal amounts of proteins from two heads were loaded for each genotype. dFMRP expression was probed with 5A11 (1:100) and detected with horseradish peroxidase-coupled secondary antibody using the chemiluminescent method (ECL kit; GE Healthcare, Little Chalfont, UK). Immunohistochemistry on the adult CNS to visualize neuronal elaborations was performed as described previously (Reeve et al., 2005).

Phenotypic and genetic interaction assays of mutations in the central ventral lateral neurons and peripheral neuromuscular junction. The dorsal axonal elaborations of ventral lateral neurons (LNv) in the brain of different *dfmr1* mutations were quantified following a protocol reported by Reeve et al. (2005). For loss-of-function (LOF) assay, brains from 1- to 3-d-old adult progeny from *dfmr1*^{113}*/TM6B* mated to each mutated *EP3517* were dissected and immunolabeled with anti-PDH (specifically labeling LNv elaborations; a kind gift from S. Bonomelli, University of West Florida, Pensacola, FL). Similarly, for gain-of-function (GOF) assays, brains of 1- to 3-d-old progeny from *Pdf–Gal4;* upstream activating sequence–green fluorescent protein (*UAS–GFP*) crossed to each mutated *EP3517* were stained anti-GFP (1:1000; Invitrogen, Carlsbad, CA). Two measurements were made for all genotypes: the distance from the point of defasciculation to the most medially extended axon, referred to as the "branch extension," and the "branching width," defined as the distance between the most dorsal arbor and the most ventral arbor. The "relative area," presented as arbitrary units in Figures 2, *E* and *J*, and 4*F*, was calculated by multiplying branch extension by branch width and normalized to brain size by the square of the posterior optic tract length as described previously (Reeve et al., 2005).

Quantifications of neuromuscular junctions (NMJs) were performed essentially as described previously (Schenck et al., 2003). At least two rounds of assays were performed per genotype, and, for each round, at least 27 NMJs were scored per genotype. In all cases, NMJs at muscle 4 of abdominal segments 1–4 were scored. Pictures of synapses were imported in an in-house developed TCS/timt software that quantifies synaptic length by automatic measurement of synaptic terminals. Statistical significance was calculated using ANOVA and the Newman–Keuls method for *post hoc* pairwise analyses.

Y2H interaction assay. A 654 bp fragment encoding the human FMRP N-terminal 218 amino acids named NT218 in this study was amplified by PCR and cloned into pGBKT7 [containing DNA-binding domain (BD) of yeast transcription factor GAL4; Clontech, Mountain View, CA]. cDNA sequences encoding human CYFIP1 (clone KIAA0068), 82-FIP (clone KIAA1321) (provided by Kazusa DNA Research Institute, Kisarazu, Japan), and FXR1 (from H. Siomi, University of Tokushima, Tokushima, Japan) were cloned into pGADT7 [containing activation domain (AD) of yeast transcription factor GAL4; Clontech]. PCR-mediated mutagenesis was used to generate specific missense mutations within the NT218 bait. Transformed yeast AH109 were plated on appropriate synthetic dropout selection medium and incubated at 30°C. All constructs were verified by sequencing and showed no self-activation. Auxotroph dependence growth and β-galactosidase activity were used to score protein–protein interactions.

Results

Isolation of mutations in *dfmr1*

Isolation of point mutations is critical for the elucidation of structure/function relationship of a target protein. For FMRP, the single amino acid mutation I304D in the K homology 2 (KH2) domain identified in a patient has provided significant insight into the functions of FMRP (Banerjee et al., 2007). To further facilitate our mechanistic understanding of FMRP, we developed an F1 screen based on the rescue of lethality caused by dFMRP overexpression (supplemental Fig. 1, available at www.jneurosci.org as supplemental material) and isolated 101 lethality suppressors. Sequencing the mutated *EP3517* chromosome identified 58 *dfmr1* mutations in 57 suppressor lines. The mutations include 26 missense mutations at 13 residues, 12 nonsense mutations, and 20 rearrangements (supplemental Fig. 2 and Table 1, available at www.jneurosci.org as supplemental material). Remarkably, all 26 missense mutations map to the N terminal 411 amino acids. Similarly, all truncations recovered start within the N-terminal 391 amino acids (supplemental Fig. 2, available at www.jneurosci.org as supplemental material). The clustering of mutations and truncations at the N terminal of dFMRP suggest a critical role for the region. Phylogenetic analysis of 41 members of FXR family comprising FMRP, FXR1, and FXR2 shows that all mutated residues are highly conserved in the FXR family across species (supplemental Table 2, available at www.jneurosci.org as supplemental material).

One potential explanation for the suppressor effects of the isolated mutations is that they all simply render the dFMRP protein untranslatable or unstable. To rule out this possibility, we performed immunochemical analyses of the suppressors (Fig. 1). Antibody staining of each mutated protein overexpressed by *Tub–Gal4* in a null background showed that many mutations,

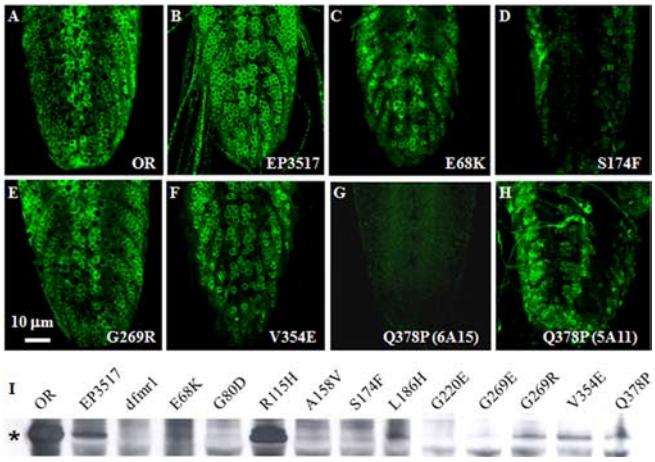

Figure 1. Immunohistochemical analyses of various mutants. To better examine the expression patterns of mutated proteins, various mutations were overexpressed driven by *Tub–Gal4* in a null background (*EP*/Tub–Gal4, dfmr1*^{50M}). ***A***, Oregon R (OR) was used as a wild-type control. ***B***, Endogenous intact dFMRP under *EP3517* was driven by *Tub–Gal4*. Expressions of mutated dFMRP driven by *Tub–Gal4* shown are E68K (***C***), S174F (***D***), G269R (***E***), V354E (***F***), and Q378P (***G***, ***H***). ***A–G*** were stained with anti-dFMRP 6A15, and ***H*** was stained with 5A11. Scale bar, 10 μm. ***I***, Expressions of *dfmr1* mutant alleles in trans over *dfmr1*^{113} in the brain were detected by Western analyses with anti-dFMRP 5A11. * indicates the band of dFMRP.

such as E68K, G269R, V354E, and Q378P, display dFMRP expression comparable with the original *EP3517* level, whereas other mutations, such as S174F, have reduced dFMRP expression (Fig. 1*A–H*), indicating that these mutations affect dFMRP expression to some extent, probably at the posttranscriptional level. Interestingly, high-level expression of Q378P was detected by monoclonal antibody 5A11 but undetectable by antibody 6A15, demonstrating that the epitope recognized by 6A15 was disrupted in the mutant. The immunostaining results were primarily confirmed by Western blot analyses (Fig. 1*I*). Together, these data argue that the expression levels do not explain the suppressor effects we observed and suggest that these alleles are functionally compromised.

Loss- and gain-of-function analyses of the missense mutations in the CNS

We chose to examine the effects of these mutations in the LNv in the central brain, because LNv play an important role in the control of circadian rhythms and are known to require dFMRP for normal axonal arborization (Dockendorff et al., 2002; Reeve et al., 2005). Specifically, *dfmr1* mutants produce an excessive defasciculation of the dorsal projections of LNv (Reeve et al., 2005). We first used this assay to study the effect of the point mutations in a null background. Because in this case the only source of dFMRP is provided by the mutated *dfmr1*, we would expect to observe a change in LNv elaboration when compared with *EP3517* control if a mutation alters the functions of dFMRP. Figure 2*A–E* shows the results of 13 different mutations examined in this assay. We found that 7 of the 13 alleles (*G80D*, *R115H*, *A158V*, *S174F*, *G220E*, *V354E*, and *Q378P*) showed defasciculation phenotypes statistically indistinguishable from the *EP3517* control, suggesting that these mutations represent wild-type or weak hypomorphic alleles. Of the remaining six alleles, five (*R47C*, *R115C*, *L186H*, *G269E*, and *R279C*) display increased axonal arborization but remain statistically less severe than the homozygous null animals, suggesting that these alleles represent moderate or strong hypomorphic mutations. Only *E68K* appears to be a null, being statistically indistinguishable from homozygous null mutants.

To further assess the functional effects conferred by the mutations, the LOF assay was followed by GOF assay. Overexpression of *dfmr1* results in axonal collapse of the dorsal LNv (Reeve et al., 2005). We expressed each of the alleles in the LNv and measured the extent of axonal collapse (Fig. 2*F–J*). We found that four alleles (*G220E*, *G269E*, *V354E*, and *Q378P*) retain significant function in this assay, suggesting they are weak hypomorphs. For three of these alleles (*G220E*, *V354E*, and *Q378P*), this is consistent with the LOF results. For *G269E*, the data are contradictory. One explanation may be that G269E affects protein level but not activity, a prediction consistent with expression analyses (Fig. 1). Of the remaining nine alleles studied, eight (*R47C*, *G80D*, *R115C*, *R115H*, *A158V*, *S174F*, *L186H*, and *R279C*) fail to cause axonal collapse, implying that they are moderate to strong hypomorphic alleles. Interestingly, we found that GOF of *E68K* causes an increase in defasciculation, phenocopying the *dfmr1* null and suggesting that this allele has either a dominant-negative or a neomorphic function. In summary, most, if not all, of the isolated mutations display a neuronal phenotype in the LOF and/or GOF assays.

Critical residues at the N terminus of FMRP for specific interactions with CYFIP1, FXR1, and 82-FIP

The N-terminal 218 residues of human FMRP, named NT218 in this study, have been shown to interact with several different proteins, including 82-FIP (Bardoni et al., 2003), NUFIP (Bardoni et al., 1999), CYFIP1, CYFIP2 (Schenck et al., 2001), and possibly FXR1 and FXR2 (Siomi et al., 1996). Remarkably, 18 of 26 missense mutations isolated are located in the NT220 of dFMRP, the equivalent of NT218 in human FMRP (supplemental Fig. 2, available at www.jneurosci.org as supplemental material). To examine whether the mutations affect protein–protein interactions, we engineered the equivalent mutations in human FMRP NT218 (R48C, E66K, C78D, R113C, R113H, A156T, A156V, S172F, L184H, and S217E) and performed Y2H analysis, because thus far no Y2H assay has been established for fly dFMRP (Schenck et al., 2003), and we found the same to be true in our hands.

In contrast, we confirmed the interactions between human FMRP NT218 and three of its partners: CYFIP1, 82-FIP, and FXR1. This allowed us to ask whether the mutations we isolated influence the binding between NT218 and its partners in the Y2H assay. As shown in Figure 3, wild-type NT218 interacts with CYFIP1 to produce well grown, blue-colored colony on selective medium, whereas some mutations in NT218 disrupt the interactions (Fig. 3*A*). Specifically, R113 and S172 are the most important for the FMRP–CYFIP1 interaction, because the two mutations completely abolished the interaction. The mutation at E66 compromised the interaction with CYFIP1 to some extent as evidenced by the pale-blue colony, whereas the rest retain wild-type level interaction with CYFIP1 (Fig. 3*A*). Conversely, mutation L184H completely abolished the interaction with FXR1, as did mutations E66K, C78D, R113C, and R113H for the interaction with 82-FIP (Fig. 3*B*). Four mutations, R48C, A156T, A156V, and S217E, however, did not affect any of the three interactions assayed. In summary, the Y2H assay reveals critical residues at the N terminus of FMRP for its specific interactions with CYFIP1, FXR1, or 82-FIP and demonstrates that different interactions require distinct amino acids.

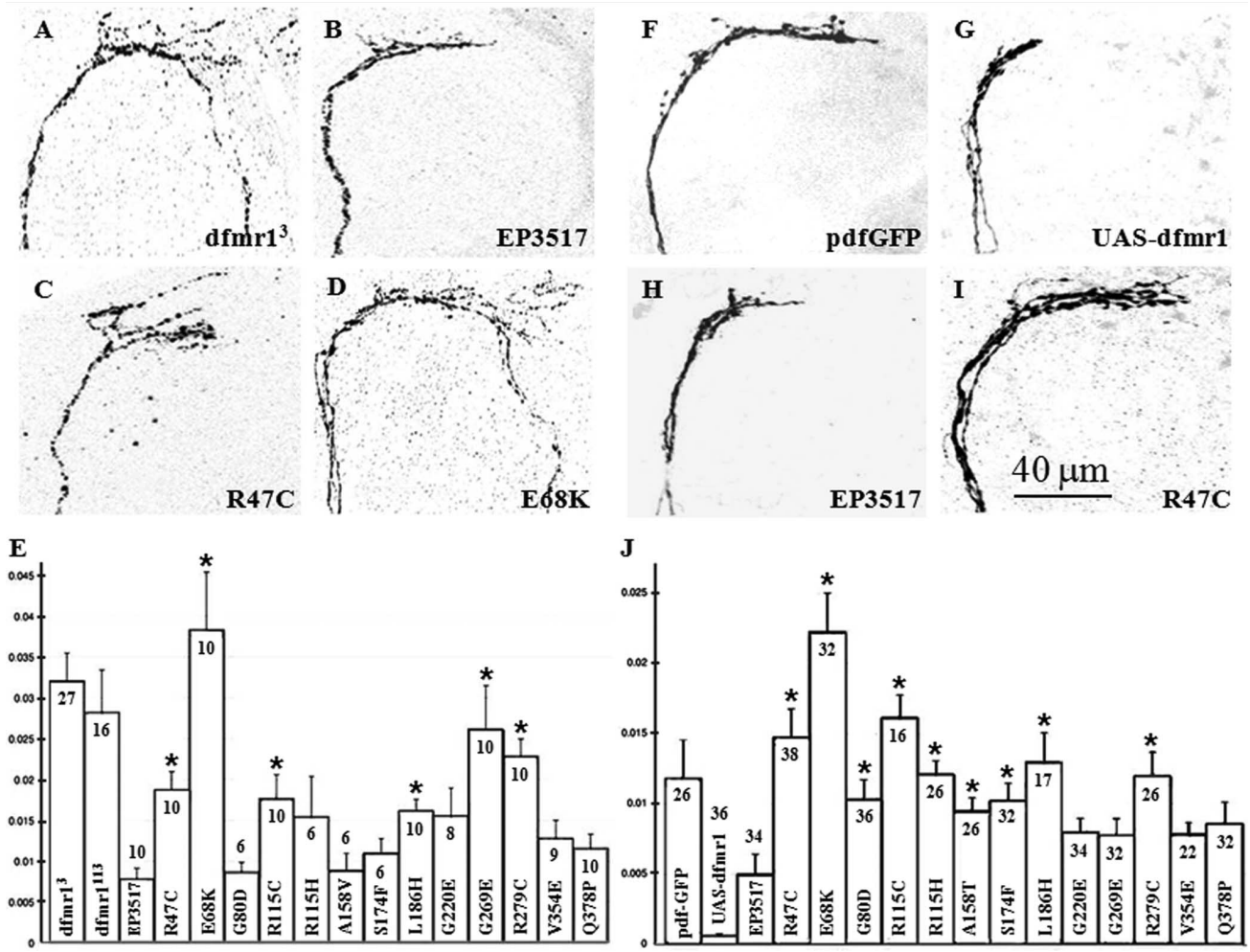

Figure 2. Decreased activities of *dfmr1* mutations in central LNv. ***A–E***, LOF assay of mutations in the LNv. ***A***, Homozygous null allele *dfmr1*^{3} shows severe defasciculation of axonal termini. Representative examples of dorsal axonal termini of mutant alleles *EP3517*, *R47C*, and *E68K* transheterozygous over *dfmr1*^{113} are shown in ***B–D***, respectively. *EP3517* shows a phenotype comparable with that of wild type (***B***). ***F–J***, GOF assay of mutations in the LNv. LNv labeled with *Pdf–GFP* are used as wild-type control (***F***). Overexpression of dFMRP by *UAS– dfmr1* (***G***) or *EP3517* (***H***) leads to decreased axonal elaboration (*UAS– dfmr1* produces a stronger phenotype than *EP3517* when driven by *Pdf–Gal4*, presumably attributable to higher expression of dFMRP) (Zhang et al., 2001). ***I*** shows the axonal termini when mutation R47C is overexpressed in LNv. ***E***, ***J***, Relative axonal elaboration area of LNv for each genotype examined. Units are arbitrary, calculated as detailed in Materials and Methods. Number of LNv quantified for each genotype from at least two rounds of assays is indicated. *$p < 0.05$, significant difference by a two-tailed *t* test with Statistica software (StatSoft, Tulsa, OK) from the control *EP3517*. Error bars are SEM.

Mutated N-terminal residues of dFMRP are critical for its *in vivo* interaction with CYFIP

The Y2H data above suggest that failure to bind some of its protein partners may be relevant to the CNS phenotypes observed with the various *dfmr1* alleles. To investigate the possibility *in vivo*, we first asked whether the mutations that abolish CYFIP binding also fail to show genetic interactions with CYFIP at the NMJ, an attractive model for studying synaptic development. CYFIP has a well established role as a dFMRP partner at NMJ (Schenck et al., 2003). Specifically, *CYFIP* and *dfmr1* LOF mutants display opposite undergrowth and overgrowth synapse, respectively (Schenck et al., 2003). Compared with the pronounced phenotypes observed in LNv, overexpression of various *dfmr1* mutations at NMJ produced a weaker effect in general (Fig. 4, compare *E*, *F*). Similar to the interaction shown in LNv (Fig. 4*F*), CYFIP and dFMRP also act antagonistically at NMJ (Fig. 4*A–E*), i.e., *CYFIP* overexpression rescues the *dfmr1* overexpression phenotype ($p = 0.0008$). Much like the co-overexpression of wild-type *dfmr1* with *CYFIP*, co-overexpression of mutant alleles carrying a mutation with interaction with CYFIP intact produced normal NMJ synapses (*R47C*, $p = 0.1$; *G80D*, $p = 0.2$; *L186H*, $p = 0.7$) (Fig. 4*A–E*). However, co-overexpression of alleles that fail to bind CYFIP did result in significant NMJ overgrowth (*E68K*, $p = 0.027$; *R115C*, $p = 0.0001$; *R115H*, $p = 0.0002$; *S174F*, $p = 0.009$) (Fig. 4*A–E*), demonstrating that the specific amino acid-mediated interaction between dFMRP and CYFIP is critical for the normal synapse development.

Thus far, no function for *CYFIP* has been shown in the adult CNS. Identification of *dfmr1* alleles that specifically fail to bind CYFIP allowed us to ask whether the dFMRP–CYFIP interaction is a general feature of dFMRP function in the nervous system. Overexpression of *CYFIP* in a wild-type background has no significant effect on LNv axonal arborization ($p = 0.2$) (Fig. 4*F*). However, *CYFIP* overexpression suppresses the effects of *EP*-mediated overexpression of wild-type *dfmr1* ($p = 1.6 \times 10^{-8}$), confirming the antagonistic interaction between *CYFIP* and *dfmr1* observed at the NMJ. In contrast, when any of the alleles whose protein products fail to bind dFMRP are co-overexpressed with *CYFIP*, we see no antagonistic effect between the two (*E68K*, $p = 0.1$; *R115C*, $p = 0.4$; *R115H*, $p = 0.08$; *S174F*, $p = 0.8$) (Fig.

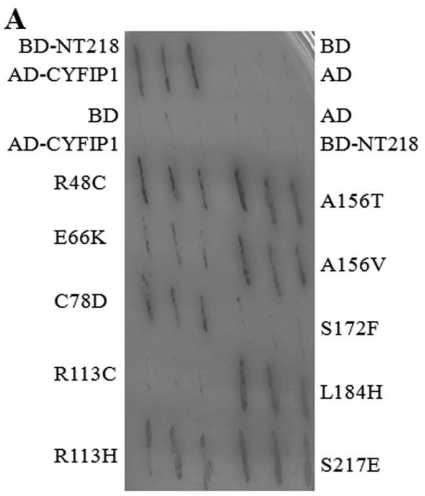

B

Mutations	CYFIP1	FXR1	82-FIP
R48C (R47C)	N	N	N
E66K (E68K)	*	N	**
C78D (G80D)	N	N	**
R113C (R115C)	**	N	**
R113H (R115H)	*	N	**
A156T (A158T)	N	N	N
A156V (A158V)	N	N	N
S172F (S174F)	**	N	N
L184H (L186H)	N	**	N
S217E (G220E)	N	N	N

Figure 3. Y2H analyses identified critical residues of FMRP for interactions with its partners. ***A***, Mutations in human FMRP N-terminal 218 amino acid peptide (NT218) disrupt its interaction with human CYFIP1. Cotransformation of two recombinant plasmids carrying the bait NT218 and the prey CYFIP1 showed robust growth of blue colony and was used as a positive control. Cotransformation of empty plasmids BD and AD, empty plasmid BD plus recombinant plasmid AD–CYFIP1, or empty plasmid AD plus recombinant plasmid BD–NT218 produced no growth of yeast on selective medium and was used as a negative control. Equivalents of the 10 mutations in human FMRP NT218, R48C, E66K, C78D, R113C, R113H, A156T, A156V, S172F, L184H, and S217E were tested. ***B***, Summary of critical FMRP residues required for specific protein–protein interactions with CYFIP1, FXR1, and 82-FIP. Equivalent mutations in dFMRP are parenthesized. * indicates moderate disruption; ** indicates complete disruption; N, no disruption.

4*F*). The loss of interaction is specific to these alleles because a strong genetic interaction is observed between *CYFIP* and mutation *V354E*, which is not in the region interacting with CYFIP ($p = 0.008$). Together, our data from *in vivo* assays at both NMJ and LNv support the conclusion that the N-terminal amino acids of FMRP involved in interaction with CYFIP are critical for its neuronal function.

Discussion

The genetic screen, in which the *EP3517* line was mutagenized to screen for mutations in the endogenous *dfmr1* downstream of the *EP* element, is efficient and productive. Because overexpression or ectopic expression of many genes can produce a simple recognizable phenotype whereas a mutation compromising the function(s) of the endogenous gene would rescue the phenotype, the screen strategy is of general utility and can be readily extended to other genes of interest, particularly those with no obvious LOF phenotypes or whose functions are unknown. Another attractive feature of the screen is that the mutations can be readily used for GOF analyses without the need of making transgenic flies carrying engineered mutations.

All the mutations isolated cluster to the N-terminal 411 residues, with no mutations found at the C-terminal 270 amino acids. Specifically, 18 of the 26 missense mutations are located at the N-terminal 220 amino acid region, mainly involved in protein–protein interaction. There are a few nonexclusive possibilities for the clustered distribution of mutations. First, the function of the C-terminal 270 amino acids may be subtle such that one residue change in the region does not sufficiently compromise dFMRP function. Indeed, this region is the least conserved in the FXR family through evolution. Second, the C-terminal 270 amino acids may not contribute to the lethality on which the genetic screen is based. Third, the functions of the four RNA binding domains NDF (N-terminal domain of FMRP), KH1, KH2, and RGG box of dFMRP may be somewhat redundant, so that disruption of one is compensated by others. Therefore, more sensitive or specific screening paradigms have to be devised to isolate mutations in the RNA binding domains. Importantly, however, most of the mutations isolated affect the neuronal functions of dFMRP in both LOF and GOF assays, demonstrating the relevance of the screen paradigm.

The FMRP NT218 interacts directly with several proteins, such as CYFIP1 (Schenck et al., 2001), FXR1/2 (Zhang et al., 1995), and 82-FIP (Bardoni et al., 2003). Our work identified critical amino acids for the specific interactions. For example, E66, R113, and S172 are vital for the interaction with CYFIP1, whereas L184, located in the coiled-coil domain (Siomi et al., 1996), is critical for the FMRP–FXR1 heterodimerization. Conversely, mutations at E66, C78, and R113 abolished the interaction with 82-FIP, which is in full agreement with the early biochemical and structural studies (Adinolfi et al., 2003; Ramos et al., 2006). Importantly, the interaction with 82-FIP and CYFIP1 shares similar residues but distinct from that with FXR1. One of the alleles we isolated, E68K, appears to interfere with the function of wild-type dFMRP. This allele also fails to bind to or interact with CYFIP, suggesting that this is not the mechanism of its function as a dominant suppressor of wild-type dFMRP. One tempting speculation is that E68K may interfere with dFMRP homomeric or heteromeric complex formation, leading to interference with the function of the wild-type allele. At any rate, it is clear that our mutational analyses identified critical residues for specific protein interactions in the N terminus of FMRP.

Finally, dFMRP has different functions in the NMJ, in which it regulates synaptogenesis, and in the central LNv, in which it regulates axonal outgrowth. However, the residues we have identified are critical for the interaction between CYFIP and dFMRP in both the LNv and NMJ, suggesting that the dFMRP–CYFIP interaction may be crucial to dFMRP function in different neuronal types and at different developmental stages. Based on the high conservation and functional importance of these and other residues in the FMRP protein, we speculate that the strong or null mutations in the critical residues of FMRP we identify here might cause rare cases of FraX patients without diagnostic CGG expansion.

References

Adinolfi S, Ramos A, Martin SR, Dal Piaz F, Pucci P, Bardoni B, Mandel JL, Pastore A (2003) The N-terminus of the fragile X mental retardation protein contains a novel domain involved in dimerization and RNA binding. Biochemistry 42:10437–10444.

Banerjee P, Nayar S, Hebbar S, Fox CF, Jacobs MC, Park JH, Fernandes JJ, Dockendorff TC (2007) Substitution of critical isoleucines in the KH domains of *Drosophila* fragile X protein results in partial loss-of-function phenotypes. Genetics 175:1241–1250.

Bardoni B, Schenck A, Mandel JL (1999) A novel RNA-binding nuclear protein that interacts with the fragile X mental retardation (FMR1) protein. Hum Mol Genet 8:2557–2566.

Bardoni B, Castets M, Huot ME, Schenck A, Adinolfi S, Corbin F, Pastore A, Khandjian EW, Mandel JL (2003) 82-FIP, a novel FMRP (fragile X mental retardation protein) interacting protein, shows a cell cycle-dependent intracellular localization. Hum Mol Genet 12:1689–1698.

Brown V, Jin P, Ceman S, Darnell JC, O'Donnell WT, Tenenbaum SA, Jin X,

Feng Y, Wilkinson KD, Keene JD, Darnell RB, Warren ST (2001) Microarray identification of FMRP-associated brain mRNAs and altered mRNA translational profiles in fragile X syndrome. Cell 107:477–487.

Davidovic L, Bechara E, Gravel M, Jaglin XH, Tremblay S, Sik A, Bardoni B, Khandjian EW (2006) The nuclear MicroSpherule protein 58 is a novel RNA-binding protein that interacts with fragile X mental retardation protein in polyribosomal mRNPs from neurons. Hum Mol Genet 15:1525–1538.

De Boulle K, Verkerk AJ, Reyniers E, Vits L, Hendrickx J, Van Roy B, Van den Bos F, de Graaff E, Oostra BA, Willems PJ (1993) A point mutation in the FMR-1 gene associated with fragile X mental retardation. Nat Genet 3:31–35.

Dockendorff TC, Su HS, McBride SM, Yang Z, Choi CH, Siwicki KK, Sehgal A, Jongens TA (2002) *Drosophila* lacking dfmr1 activity show defects in circadian output and fail to maintain courtship interest. Neuron 34:973–984.

Grigliatti TA (1998) Mutagenesis. In: *Drosophila*, a practical approach, Ed 2 (Roberts DB, ed), pp 55–83. Oxford, UK: Oxford UP.

Hammond LS, Macias MM, Tarleton JC, Shashidhar Pai G (1997) Fragile X syndrome and deletions in FMR1: new case and review of the literature. Am J Med Genet 72:430–434.

Koekkoek SK, Yamaguchi K, Milojkovic BA, Dortland BR, Ruigrok TJ, Maex R, De Graaf W, Smit AE, VanderWerf F, Bakker CE, Willemsen R, Ikeda T, Kakizawa S, Onodera K, Nelson DL, Mientjes E, Joosten M, De Schutter E, Oostra BA, Ito M, De Zeeuw CI (2005) Deletion of FMR1 in Purkinje cells enhances parallel fiber LTD, enlarges spines, and attenuates cerebellar eyelid conditioning in Fragile X syndrome. Neuron 47:339–352.

Leyssen M, Hassan BA (2007) A fruitfly's guide to keeping the brain wired. EMBO Rep 8:46–50.

Michel CI, Kraft R, Restifo LL (2004) Defective neuronal development in the mushroom bodies of *Drosophila* fragile X mental retardation 1 mutants. J Neurosci 24:5798–5809.

Morales J, Hiesinger PR, Schroeder AJ, Kume K, Verstreken P, Jackson FR, Nelson DL, Hassan BA (2002) *Drosophila* fragile X protein, DFXR, regulates neuronal morphology and function in the brain. Neuron 34:961–972.

O'Donnell WT, Warren ST (2002) A decade of molecular studies of fragile X syndrome. Annu Rev Neurosci 25:315–338.

Pan L, Zhang YQ, Woodruff E, Broadie K (2004) The *Drosophila* fragile X gene negatively regulates neuronal elaboration and synaptic differentiation. Curr Biol 14:1863–1870.

Ramos A, Hollingworth D, Adinolfi S, Castets M, Kelly G, Frenkiel TA, Bardoni B, Pastore A (2006) The structure of the N-terminal domain of the fragile X mental retardation protein: a platform for protein-protein interaction. Structure 14:21–31.

Reeve SP, Bassetto L, Genova GK, Kleyner Y, Leyssen M, Jackson FR, Hassan BA (2005) The *Drosophila* fragile X mental retardation protein controls actin dynamics by directly regulating profilin in the brain. Curr Biol 15:1156–1163.

Schenck A, Bardoni B, Moro A, Bagni C, Mandel JL (2001) A highly conserved protein family interacting with the fragile X mental retardation protein (FMRP) and displaying selective interactions with FMRP-related proteins FXR1P and FXR2P. Proc Natl Acad Sci USA 98:8844–8849.

Schenck A, Bardoni B, Langmann C, Harden N, Mandel JL, Giangrande A (2003) CYFIP/Sra-1 controls neuronal connectivity in *Drosophila* and links the Rac1 GTPase pathway to the fragile X protein. Neuron 38:887–898.

Siomi MC, Zhang Y, Siomi H, Dreyfuss G (1996) Specific sequences in the fragile X syndrome protein FMR1 and the FXR proteins mediate their binding to 60S ribosomal subunits and the interactions among them. Mol Cell Biol 16:3825–3832.

Wan L, Dockendorff TC, Jongens TA, Dreyfuss G (2000) Characterization of dFMR1, a *Drosophila melanogaster* homolog of the fragile X mental retardation protein. Mol Cell Biol 20:8536–8547.

Zhang Y, O'Connor JP, Siomi MC, Srinivasan S, Dutra A, Nussbaum RL, Dreyfuss G (1995) The fragile X mental retardation syndrome protein interacts with novel homologs FXR1 and FXR2. EMBO J 14:5358–5366.

Zhang YQ, Broadie K (2005) Fathoming fragile X in fruit flies. Trends Genet 21:37–45.

Zhang YQ, Bailey AM, Matthies HJ, Renden RB, Smith MA, Speese SD, Rubin GM, Broadie K (2001) *Drosophila* fragile X-related gene regulates the MAP1B homolog Futsch to control synaptic structure and function. Cell 107:591–603.

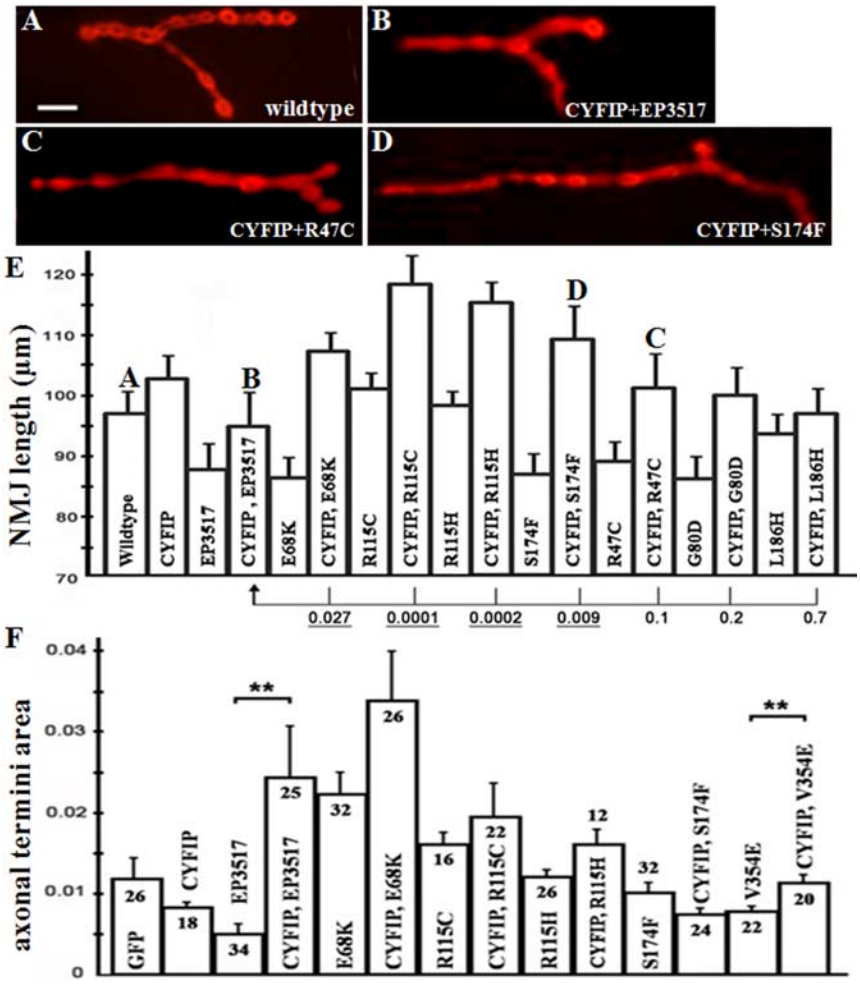

Figure 4. *In vivo* interaction assay between *CYFIP* and *dfmr1* mutations. ***A–D***, Representative NMJ at muscle 4 labeled with a postsynaptic marker anti-Disc Large of different genotypes. Pan-neuronal *elav–Gal4* driver as a wild-type control (***A***). *elav–Gal4* driven co-overexpression of *CYFIP* and *EP3517* (***B***), *CYFIP* and *R47C* (***C***), and *CYFIP* and *S174F* (***D***). Scale bar, 10 μm. ***E***, NMJ quantifications of either overexpression of mutated *dfmr1* alone or co-overexpression of mutated *dfmr1* and *CYFIP* driven by *elav–Gal4*. Error bars indicate SEM ($n > 50$). p values derived from comparison between co-overexpression of wild-type *dfmr1* and *CYFIP* and co-overexpression of mutated *dfmr1* and *CYFIP* are given with significant changes underlined ($p < 0.05$). ***F***, Interaction of *dfmr1* and *CYFIP* in LNv. As a positive control, the collapsed phenotype seen with expression of *EP3517* can be rescued with coexpression of *CYFIP* ($p = 1.6 \times 10^{-8}$). In contrast, no significant antagonistic interaction were seen between expression of mutant alleles with CYFIP interaction disrupted alone and its co-overexpression with *CYFIP* (for *E68K*, $p = 0.1$; *R115C*, $p = 0.4$; *R115H*, $p = 0.08$; *S174F*, $p = 0.8$). As an additional control, co-overexpression of *CYFIP* with mutant allele *V354E*, which has the mutation outside of the protein interaction domain, was seen to interact with *CYFIP*, with a statistically significant antagonistic effect ($p = 0.008$). *y*-Axis indicates arbitrary units representing axonal elaboration area of LNv. Number of neurons quantified for each genotype is noted. $^{**}p < 0.01$, significant difference between the pair. Error bars are SEM.